Article

Cell Reports

KDEL Receptors Assist Dengue Virus Exit from the Endoplasmic Reticulum

Graphical Abstract

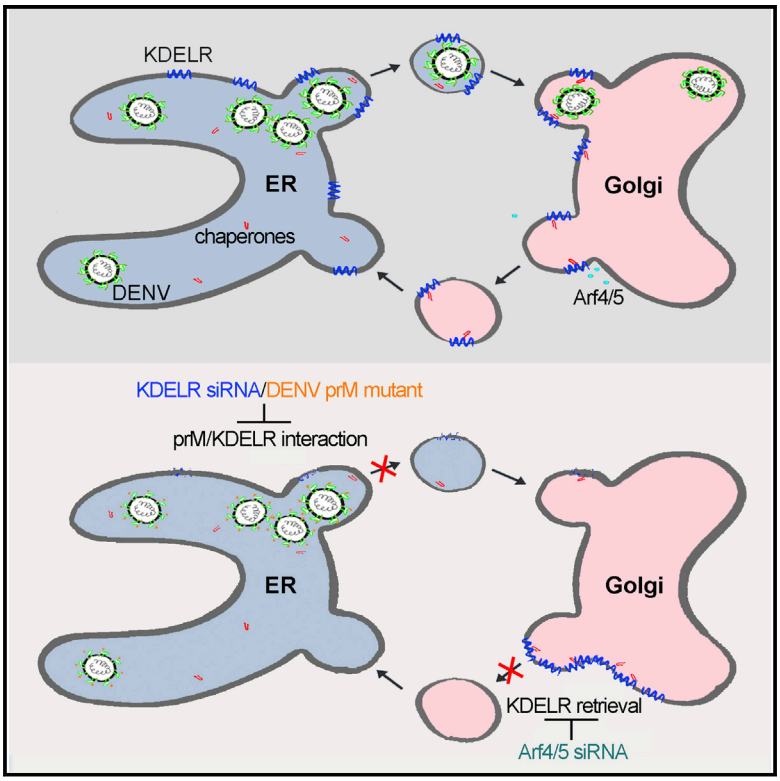

Highlights

- Depletion of KDELR by siRNA reduces egress of DENV progeny
- DENV1-3 structural protein prM interacts with KDELR in the ER
- KDELR/prM interaction requires three positively charged amino acids at N terminus of prM
- Disrupting this interaction inhibits DENV1 RSPs transport from the ER to the Golgi

Authors

Ming Yuan Li, Marc Grandadam, ..., Roberto Bruzzone, Pei Gang Wang

Correspondence

bruzzone@hku.hk (R.B.), pgwang@163.com (P.G.W.)

In Brief

Viral receptors are key host factors for virion entry; however, it is not known whether trafficking and secretion of progeny virus also requires host intracellular receptors. Li et al. show that dengue virus (DENV) interacts with host KDEL receptors (KDELR) in the ER. Depleting KDELR, disrupting DENV/KDELR interaction or blocking KDELR cycling between the ER and Golgi reduce virus release, resulting in virus accumulation in the ER. The authors propose that KDELR functions as intracellular receptors to assist in DENV exit from the ER.

Li et al., 2015, Cell Reports *10*, 1496–1507
March 10, 2015 ©2015 The Authors
http://dx.doi.org/10.1016/j.celrep.2015.02.021

OPEN ACCESS
CellPress

Cell Reports
Article

KDEL Receptors Assist Dengue Virus Exit from the Endoplasmic Reticulum

Ming Yuan Li,[1] Marc Grandadam,[2] Kevin Kwok,[1] Thibault Lagache,[3,4] Yu Lam Siu,[1] Jing Shu Zhang,[1] Kouxiong Sayteng,[2] Mateusz Kudelko,[1,5] Cheng Feng Qin,[6] Jean-Christophe Olivo-Marin,[3,4] Roberto Bruzzone,[1,4,*] and Pei Gang Wang[1,7,*]

[1]HKU-Pasteur Research Pole and Centre of Influenza Research, School of Public Health, LKS Faculty of Medicine, The University of Hong Kong, Hong Kong SAR, China
[2]Institut Pasteur du Laos, Vientiane, Lao PDR
[3]Unité d'Analyse d'Images Biologiques, CNRS URA 2582, Department of Cell Biology and Infection, Institut Pasteur, 75015 Paris Cedex, France
[4]Department of Cell Biology and Infection, Institut Pasteur, 75015 Paris Cedex, France
[5]Department of Biochemistry, LKS Faculty of Medicine, The University of Hong Kong, Hong Kong SAR, China
[6]Department of Virology, Beijing Institute of Microbiology and Epidemiology, Beijing 100071, PR China
[7]Key Laboratory of Protein and Peptide Pharmaceuticals, Institute of Biophysics, Chinese Academy of Sciences, Beijing 100101, PR China
*Correspondence: bruzzone@hku.hk (R.B.), pgwang@163.com (P.G.W.)
http://dx.doi.org/10.1016/j.celrep.2015.02.021

SUMMARY

Membrane receptors at the surface of target cells are key host factors for virion entry; however, it is unknown whether trafficking and secretion of progeny virus requires host intracellular receptors. In this study, we demonstrate that dengue virus (DENV) interacts with KDEL receptors (KDELR), which cycle between the ER and Golgi apparatus, for vesicular transport from ER to Golgi. Depletion of KDELR by siRNA reduced egress of both DENV progeny and recombinant subviral particles (RSPs). Coimmunoprecipitation of KDELR with dengue structural protein prM required three positively charged residues at the N terminus, whose mutation disrupted protein interaction and inhibited RSP transport from the ER to the Golgi. Finally, siRNA depletion of class II Arfs, which results in KDELR accumulation in the Golgi, phenocopied results obtained with mutagenized prME and KDELR knockdown. Our results have uncovered a function for KDELR as an internal receptor involved in DENV trafficking.

INTRODUCTION

Dengue, a mosquito-borne viral infection endemic in over 100 countries, is caused by four serotypes of dengue virus (DENV1–4). In addition to a febrile, influenza-like illness, severe dengue represents a public health concern in Asia and South America where it is a major cause of death across all ages (Guzman et al., 2010; Messina et al., 2014). Despite the global burden of disease, there is no specific treatment and, therefore, a molecular understanding of host-pathogen interactions during the cellular life cycle is needed to guide the development of effective drugs (Guzman et al., 2010).

DENV has two structural glycoproteins: pre-membrane (prM) and envelope (E) (Kuhn et al., 2002); E mediates interaction with cellular receptor(s) for viral attachment and entry (Chen et al., 1997), whereas prM assists E in its correct folding (Courageot et al., 2000) and protects it from pre-fusion in the acidic environment of the secretory pathway (Zhang et al., 2003). Assembly of DENV occurs at the ER and requires interaction of prM and E (Mukhopadhyay et al., 2005; Pryor et al., 2004). Nascent virions bud into the lumen of the ER, accumulating in dilated cisternae oriented toward the *cis*-Golgi, and are translocated to the Golgi via trafficking vesicles (Welsch et al., 2009). In the trans-Golgi network (TGN), prM protein is cleaved by the cellular protease furin, resulting in the release of the pr peptide and formation of infectious DENV (Li et al., 2008; Yu et al., 2008). Besides mature virions, non-infectious recombinant subviral particles (RSP) can be produced by cells expressing DENV prME proteins (Mukhopadhyay et al., 2005). Dengue RSP traffic along the same compartments as infectious DENV, and represent a safe and convenient tool for the study of virus-host interactions during secretion (Wang et al., 2009).

Although DENV egress has been studied for many years, most cellular targets identified in high-throughput screens have not been mapped to the secretory pathway (Sessions et al., 2009). We recently identified two cellular factors, ADP-ribosylation factor 4 and 5 (Arf4 and Arf5), which are involved in secretion of DENV progeny (Kudelko et al., 2012). Because Arfs play an important role in the recruitment of coat proteins necessary for the formation of trafficking vesicles (D'Souza-Schorey and Chavrier, 2006), our results indicate that Arf4+5 are acting at an early step of DENV secretion (Kudelko et al., 2012). The specific involvement of Arfs, which are dispensable factors for the constitutive pathway, in DENV trafficking suggested that the virus uses a more complex machinery and that other cellular factors besides Arf4+5 might also assist to exit the infected cell.

Sorting of cargo is dependent on molecular recognition, a process equivalent to receptor-ligand interactions; however, it is not known whether newly formed DENV exploits host factors

to move along the secretory pathway. Intriguingly, depletion of Arf4+5 has also been reported to inhibit the retrograde trafficking of KDEL receptor (KDELR) from Golgi to ER (Volpicelli-Daley et al., 2005). The three KDELR members (KDELR1–3) identified (Hsu et al., 1992; Lewis and Pelham, 1990, 1992b; Raykhel et al., 2007) are transmembrane proteins cycling between ER and Golgi apparatus to prevent leakage of ER-resident proteins, such as chaperones, and retrieve them back to the ER (Lewis and Pelham, 1990). As KDELR binding to cargo through a C terminus KDEL motif occurs only in the Golgi apparatus, we investigated their possible involvement in translocation of DENV from assembly and budding sites in the ER to the Golgi.

We show here that KDELR1 and KDELR2 play crucial roles for DENV1–3, but not DENV4 secretion. KDELR interacted with DENV through three positively charged amino acids at the N terminus of prM. DENV secretion could be blocked either by depletion of KDELR, arrest of KDELR cycle, or disruption of prM/KDELR interaction. Under these conditions, progeny DENV accumulated in the ER and did not reach the Golgi apparatus. Our results demonstrate that KDELRs function as luminal receptors for DENV transport along the secretory pathway.

RESULTS

KDELR Interact with prM of DENV1

We previously demonstrated that depletion of Arf4+5 inhibited DENV1 and RSP release without disrupting constitutive secretion (Kudelko et al., 2012). To gain insight into the underlying molecular mechanism, we investigated the role of KDELRs, which accumulate in a peri-nuclear region and are not recycled back to the ER following Arf4+5 depletion (Volpicelli-Daley et al., 2005). All three KDELR identified thus far were detected by RT-PCR in our cellular models (Figure 1A). We observed a redistribution of KDELR in cells stably transfected with prME (HeLa-prME-DENV1), with an apparent reduction of co-staining with the *cis*-Golgi marker GM130 in comparison to parental HeLa (Figure 1B). Moreover, partial co-localization of E and KDELR was observed in either HeLa-prME-DENV1 or Vero E6 cells infected with DENV1 (Figure 1C). Although a prominent aggregation of E protein was seen in HeLa-prME-DENV1 (Figure 1C), this did not reflect different distribution, as prME co-localized with ER marker in both cell lines (data not shown). Similar results were obtained in cells co-transfected with DENV1 prME and KDELR1-RFP (Figure S1A). These observations suggested the participation of KDELRs in DENV1 life cycle.

We next performed co-immunoprecipitation (coIP) using either dengue patient serum (DPS), containing antibodies recognizing prME (Kudelko et al., 2012), or normal human serum (NHS) as control. Pellets of coIPs were analyzed with western blotting (WB) with antibodies recognizing either prM and E, or the three KDELR. prME glycoprotein was specifically pulled down by DPS, but not NHS (Figure 1D). Although expression levels were comparable, KDELR were detected only in pellets from HeLa-prME-DENV1, but not parental cells (Figure 1D). Similarly, when coIP was performed with replication-competent DENV1, a strong signal for KDELR was visible only in pellets from infected Vero E6 cells (Figure 1E), confirming a biochemical interaction between KDELR and prME. KDELR were also precipitated from lysates of stable cell lines producing RSP of DENV2 and DENV3, but not DENV4 (Figure 1F), suggesting a certain degree of specificity between serotypes.

To investigate which portion of the envelope glycoprotein, prM or E, was responsible for interaction with KDELR, the 4G2 monoclonal antibody, recognizing E but not prM, was used in coIP assays. KDELR were not present in pellets obtained following incubation with the 4G2 monoclonal (Figure 1G), indicating that E was not responsible for interaction with KDELR. These observations were corroborated by detecting KDELR in coIP pellets with the prM-6.1 monoclonal antibody, which recognizes prM but not E protein (Figure 1G). The biochemical interaction between prM and KDELR was further validated by coIP in 293T cells co-transfected with prME and KDELR1-myc (Figure S1B). To conclusively define the role of prM and E in the interaction with KDELR, we used two complementary approaches. First, glutathione S-transferase (GST)-fusion proteins with truncated prM fragments were incubated with lysates of cells stably transfected with KDELR1-myc. Pull-down assays showed that prM-ΔTM, the full-length protein without the transmembrane domain (130 amino acids), pr fragment (91 amino acids) and the first 40 amino acids of prM sequence (pr40) could all interact with KDELR (Figure 1H), revealing that the amino-terminal domain of prM was sufficient to mediate interaction with KDELR. Second, mature and immature RSP were used as baits to pull down KDELR from cell lysates. Immature RSP were produced in the presence of NH_4Cl, an inhibitor of furin, and thus contained full-length prM and E (Wang et al., 2009). Mature RSP were produced from immature RSP after in vitro cleavage by furin, which released the pr fragment and, therefore, contained only E and M. KDELR could only be detected when immature, but not mature RSP were incubated with HeLa cell lysates and then subjected to immune-precipitation (Figure 1I). These results demonstrate that interaction with KDELR was dependent on the N-terminal pr fragment of prM, as its release from immature RSP prevented pull-down of KDELR.

KDELR Knockdown Reduces Secretion of DENV RSP

To investigate the impact of the interaction between KDELR and prM on DENV1 life cycle, we transfected HeLa-prME-DENV1 cells that constitutively secrete RSP with siRNAs targeting all three KDELR; this resulted in an 81% ± 4% (n = 3) reduction of KDELR protein (Figure 2A). Silencing of KDELR did not affect cell viability, as determined by propidium iodide staining (Figure S2A), or morphology (Figure S2B). Our results show that depletion of KDELR had no effect on intracellular E protein expression, but significantly reduced RSP secretion (Figure 2A).

To test whether the effect of KDELR on RSP release was part of a general mechanism that would interfere with the constitutive secretory pathway, we analyzed ssHRP release (Bard et al., 2006; Kudelko et al., 2012). No difference was observed in secreted ssHRP or intracellular HRP activity after downregulation of KDELR or Arf4+5, when compared to controls (Figure 2B). In contrast, secretion of ssHRP-KDEL occurred only in cells treated with KDELR or Arf4+5 siRNAs, confirming that both manoeuvers had interfered with retrieval of KDELR to the ER, resulting in a parallel reduction of HRP activity in cell lysates (Figure 2B). These

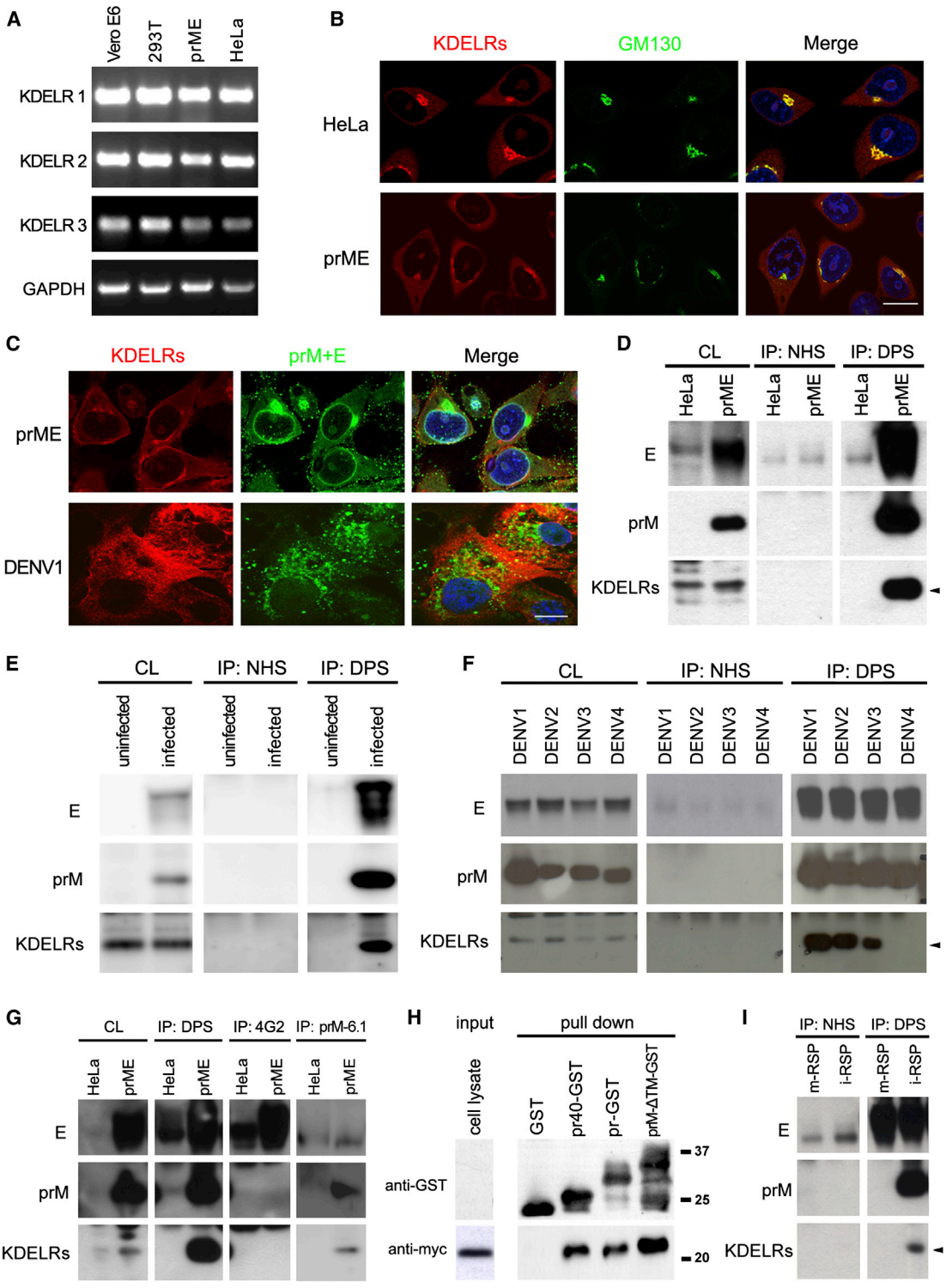

Figure 1. KDELR Interact with prM Glycoprotein of DENV1-3

(A) Expression of all three KDELR (KDELR1–3) isoforms was detected by RT- PCR in the cell lines used in our experiments. GAPDH was used as control for the amount of cDNA template.

(B) In contrast to parental HeLa, endogenous KDELR (red) did not accumulate in *cis*-Golgi (anti-GM130, green) in cells stably expressing prME of DENV1 (prME).

(C) Endogenous KDELR (red) and DENV1 prM and E proteins (revealed with an anti-prME polyclonal antibody, green) were partially co-localized in HeLa-prME-DENV1 (prME, top) and DENV1 infected Vero E6 cells (MOI = 0.1, bottom); scale bar represents10 μm.

(legend continued on next page)

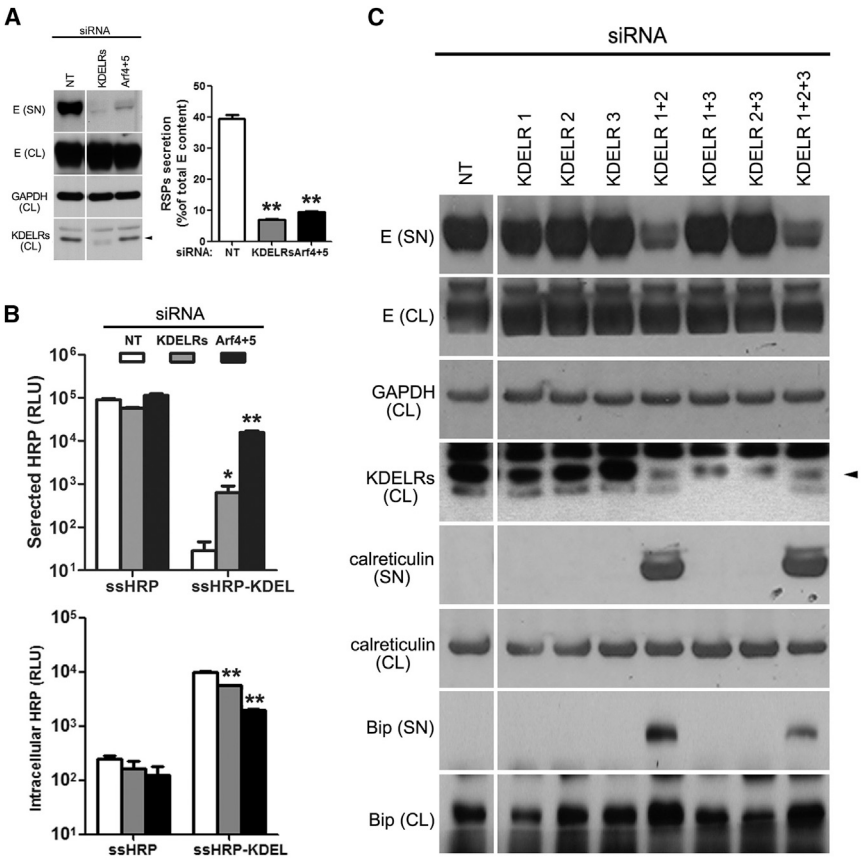

Figure 2. KDELR Knockdown Reduces Secretion of DENV1 RSP

(A) HeLa-prME-DENV1 cells were transfected with siRNAs against all three KDELR isoforms, Arf4/Arf5 (Arf4+5), and non-targeting (NT). Knockdown efficiency was determined with WB. E protein in supernatants (SN) and cell lysates (CL) was depicted by WB, quantified by densitometry and RSPs secretion was expressed as the percentage of E protein detected in SN relative to the total amount (SN+CL). GAPDH was used as the loading control across wells. Results are means ± SD (n = 3, right).

(B) KDELR downregulation did not inhibit constitutive secretion. HeLa cells expressing a secreted form of horseradish peroxidase (ssHRP) or ssHRP-KDEL were transfected with siRNAs targeting KDELR (gray) or Arf4+5 (black). Secreted and intracellular ssHRP horseradish peroxidase activity was measured in both SN and CL. Results are means ± SD (n = 3).

(C) HeLa-prME-DENV1 cells were transfected with siRNAs targeting KDELR either individually or in various combinations. SN and CL were analyzed by WB to assess RSP secretion (anti-E), release of chaperones (anti-Bip and anti-calreticulin) and knockdown of KDELR (KR-10). GAPDH was used as the loading control across wells. Results are representative of three independent experiments. *$p < 0.05$; **$p < 0.005$ versus control (NT) siRNAs.

results demonstrate that KDELR specifically assisted RSP release and their involvement was independent of perturbation of the constitutive pathway.

To study the role of individual KDELR on DENV1 secretion, siRNAs targeting individual KDELR were transfected into HeLa-prME-DENV1 in various combinations. Although individual knockdowns of KDELR did not induce significant changes, KDELR1+2 and KDELR1+2+3 siRNAs drastically reduced RSP release (Figure 2C), indicating both a crucial role for KDELR1/KDELR2 and functional compensation between these two isoforms.

As KDELR depletion caused the release of KDEL-carrying proteins (Figure 2B), the effect on DENV1 secretion might have been simply due to shortage of chaperones, such as Bip and calreticulin, which are required for the assembly of DENV (Limjindaporn et al., 2009). This possibility was excluded by showing that, although both proteins were detected in supernatants from cells treated with KDELR1+2 and KDELR1+2+3 siRNAs, their amount in cell lysates was not appreciably modified when compared to controls (Figure 2C). These experiments also show that only KDELR1 and KDELR2 were necessary for chaperones retention in the ER (Figure 2C), suggesting that KDELR isoforms assisting DENV1 secretion and retrieving ER-resident proteins were the same. Since KR-10 antibody could not distinguish between the three KDELR (Figure 2C), the efficacy of siRNA targeting each isoform was independently verified in cells expressing tagged KDELR1-3 (Figure S2C) (Kudelko et al., 2012).

(D) KDELR were pulled down with dengue patient serum (DPS) from HeLa-prME-DENV1 (prME) but not parental HeLa cells. Normal human serum (NHS) was used as control. Cell lysates (CL) or pellets following immunoprecipitation (IP) were analyzed with WB. In WB of IP pellets revealed with anti-E antibody, the weak bands detected with NHS (middle) corresponded to IgG heavy chains of the IP antibody.

(E) CoIP with DPS pulled down KDELR from lysates of DENV1 infected Vero E6 (5 days postinfection; MOI = 0.01) but not uninfected cells.

(F) KDELR were precipitated by coIP from cells stably expressing prME of DENV1–3, but not DENV4. Cell lysates (CL) from HeLa-prME-DENV1–4 (labeled DENV1–4 on top of the gel) were collected for coIP assay as described above. Whereas DPS could pull down comparable amounts of prM and E proteins of DENV1–4, KDELRs were only detected in DENV1–3 IP pellets.

(G) KDELR were not pulled down by coIP using antibody 4G2, which recognizes E but not prM. In contrast, KDELRs were detected when the antibody prM-6.1, which recognizes prM but not E, was used.

(H) GST-fusion proteins of prM fragments pulled down c-*myc*-tagged KDELR. Cell lysates (input) and pull-down pellets were revealed with WB with anti-GST and anti-c-*myc* antibodies.

(I) Immature (i) but not mature (m) RSP pull down KDELR. HeLa cells lysates were incubated with purified mature or immature RSP and then subjected to IP using DPS or NHS.

Results are representative of at least three independent experiments.

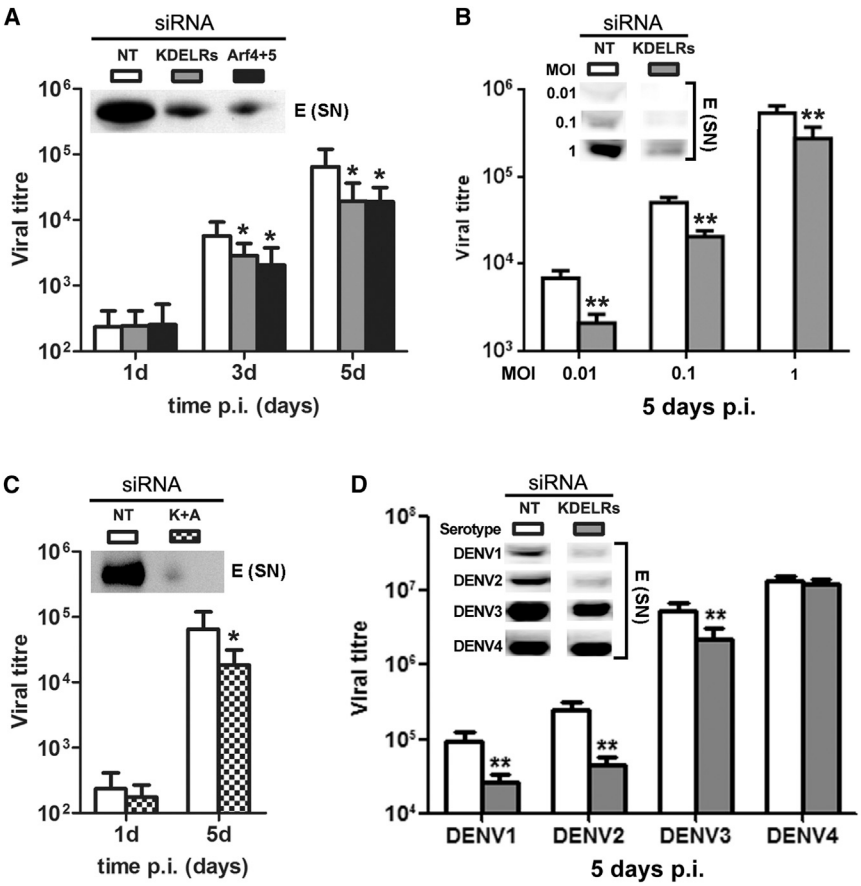

Figure 3. KDELR Knockdown Reduces DENV Egress

(A) KDELR knockdown reduced DENV1 virus titer. Vero E6 cells were transfected with KDELR siRNAs (gray) before being challenged with DENV1 (MOI = 0.1). Non-targeting (NT, open) and Arf4+5 (black) siRNAs served as negative and positive controls, respectively. Viral titers were measured at 1, 3, and 5 days postinfection (p.i.). Results are means ± SD (n = 3). SN were collected at 5 days p.i. and E protein was detected by WB (inset).

(B) siRNA-treated Vero E6 cells were challenged with DENV1 at increasing MOIs and viral titers were measured 5 days p.i. Results are means ± SD (six to eight observations from two independent experiments). Inset shows WB of E protein in SN at 5 days p.i.

(C) The effect of simultaneous knockdown of KDELR and Arf4+5 (K+A, hatched) on DENV1 titers was measured at 1 and 5 days p.i. Results are means ± SD (n = 3). E protein in SN was detected by WB (inset).

(D) KDELR knockdown inhibited secretion of DENV2 and DENV3, but not DENV4 progeny virus. Cells were treated as described in (A) and infected at an MOI of 0.1. Progeny virus was measured at 5 days p.i. Results are means ± SD of three to four measurements from one of two independent experiments with similar results. E protein in SN was detected in parallel by WB (inset). *$p < 0.05$; **$p < 0.005$ versus control (NT) siRNAs.

KDELR Knockdown Reduces DENV Egress

We next investigated the effect of KDELR knockdown on replicative DENV1 in Vero E6 cells. At 3 and 5 days post-infection, titers of progeny virus from KDELR-depleted cells were significantly lower than those of control cells (Figure 3A). A similar reduction was also found in cells treated with Arf4+5 siRNA (Figure 3A; Kudelko et al., 2012). Besides viral titers, a drastic reduction of E protein levels was detected in supernatants from cells treated with KDELR or Arf4+5 siRNAs (Figure 3A, inset). A significant decrease of DENV1 egress was also observed in KDELR-depleted cells challenged with different MOI (Figure 3B). In further experiments, Vero E6 cells were co-transfected with KDELR and Arf4+5 siRNAs before being challenged with DENV1. Measurements of progeny virus titer and E protein showed a similar inhibition in comparison to control cells (Figure 3C), suggesting that KDELR and Arf4+5 converged on the same pathway to interfere with DENV1 secretion. The efficiency of siRNA treatments was verified by WB (Figure S3A). We next tested in parallel the impact of KDELR silencing on all four DENV serotypes and observed a significant reduction of viral progeny titer for both DENV2 and DENV3, but not DENV4 (Figure 3D), consistent with the finding that only DENV1–3 were able to interact with KDELRs (see Figure 1F). Control experiments confirmed that siRNA treatment did not affect cell morphology and viability (Figures S3B and S3C). We then investigated the impact of KDELRs on egress of West Nile Virus (WNV), another flavivirus transmitted by mosquito vectors (Campbell et al., 2002) and found that viral progeny titer from KDELR-depleted cells was not different from that measured in controls ($5.6 \pm 2.5 \times 10^9$ versus $6.7 \pm 1.6 \times 10^9$, respectively; mean ± SD of n = 6 from two independent experiments). These results are in keeping with our previous findings that different flaviviruses budding in the ER do not rely on the same cellular factors for intracellular traffic (Kudelko et al., 2012).

Finally, to exclude that the effect of KDELR knockdown on DENV1 egress was the consequence of changes in the early stages of the virus life cycle, we infected Vero E6 cells for 18 hr, less than the minimum time required for newly formed virions to be released from infected cells (Lindenbach and Rice, 2001). Our experiments show that similar amounts of viral RNA were measured in cells pre-treated with either KDELR or control siRNAs (Figure S3D), indicating that KDELR knockdown had no effect on early stages of the viral life cycle.

prM/KDELR Interaction Occurs in the ER

Because KDELR are shuttling between ER and Golgi apparatus (Lewis and Pelham, 1992a; Raykhel et al., 2007), we designed experiments to ascertain in which compartment the prM/KDELR interaction occurred. We found that, in cells treated with Arf4+5 siRNA-, almost all KDELR signal was co-localized with GM130, whereas in controls only a small fraction exhibited co-staining with the *cis*-Golgi marker (Figure 4A). Therefore, we took

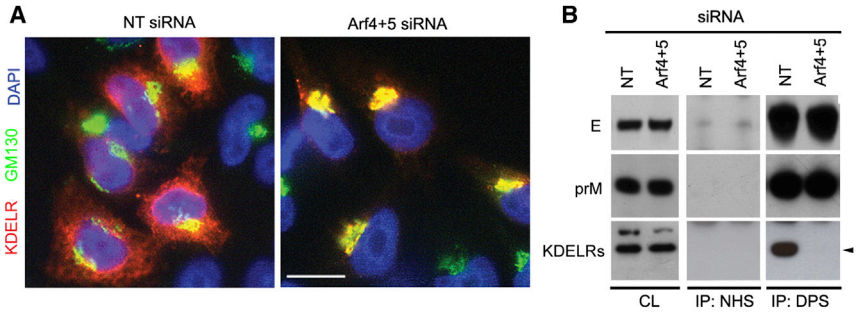

Figure 4. prM/KDELR Interaction Occurs in the ER

(A) Depletion of Arf4+5 by siRNA blocked retrieval of KDELR from Golgi. HeLa cells expressing KDELR1-RFP (red) were transfected with Arf4+5 siRNA and stained with anti-GM130 antibody (green). Non-targeting (NT) siRNA was used as control. Scale bar represents 10 μm.

(B) KDELR sequestered in Golgi were not precipitated by dengue patient serum (DPS). HeLa-prME-DENV1 cells transfected with Arf4+5 or NT siRNAs were subjected to coIP using DPS or normal human serum (NHS). Cell lysates (CL) and pellets from immunoprecipitation (IP) were analyzed by WB. Results are representative of three independent experiments.

advantage of this observation, which identifies the *cis*-Golgi as the peri-nuclear region where KDELR was sequestered following Arf4+5 depletion (Volpicelli-Daley et al., 2005), to perform coIP in Arf4+5 knockdown cells. Despite similar expression levels in all experimental conditions, KDELR could be precipitated only from control, but not Arf4+5 depleted cells (Figure 4B), indicating that prM/KDELR interaction occurred in the ER.

H2, R19, and K21 Are Key Residues for prM/KDELR Interaction

To identify the putative region of prM interacting with KDELR, we analyzed the N-terminal sequence of the pr fragment and noted a high proportion (seven of 26 residues) of positively charged amino acids (Figure 5A) that were conserved in DENV1–3, whereas substitutions at residues H2 and H11 were present in DENV4 (Figure S4A). To test the role of this cluster of basic residues we generated prME-DENV1 constructs with neutral amino acids substitutions (Figure 5A). Mutations did not affect expression of KDELR, prM, and E, with the exception of R6S, which reduced the levels of both viral proteins when compared to wild-type prME (Figure 5B, upper; and Figure S4B). Cell lysates were subjected to coIP and the ability of mutant prM to interact with KDELR was determined by calculating the ratio between precipitated KDELR and prM, which was then normalized to that measured for wild-type prM (Figure 5B, middle). H2L, R6S, R19S, and K21T significantly reduced prM binding to KDELR (Figure 5B, lower) and release of RSP (Figure 5C), demonstrating a positive correlation between prM/KDELR interaction and RSP secretion.

prM/E interaction is critical for the formation of DENV (Courageot et al., 2000): prM functions as the chaperone of E and its R6 residue is predicted to be important for both interaction and viral assembly (Li et al., 2008). To test the effect of the mutated constructs on prM/E interaction, we performed coIP assays on lysates of 293T cells and found that similar levels of prM protein could be precipitated for all mutants with the exception of R6S (Figure S4B). These observations, while confirming the predicted involvement of R6 (Li et al., 2008), demonstrate that none of the other mutated residues was involved in the interaction between prM and E.

Based on the results of coIP (Figure 5B) and RSP secretion (Figure 5C), we generated a triple mutant (H2L/R19S/K21T) designated hereinafter as "Triple." The Triple mutation did not alter the ability to bind Arf4 and Arf5 (Figure S5), but abrogated interaction with KDELRs (Figure 5D) and blocked the secretion of RSP by 90% (Figure 5E), demonstrating the crucial role of H2, R19, and K21 residues for prM interaction with KDELR and DENV1 secretion.

Triple Mutant prME Forms RSP and Is Translocated within the ER

To exclude the possibility that disruption of prM/KDELR interaction had compromised the assembly and formation of viral particles, we performed freeze-and-thaw (F&T) experiments, which have been shown to release intracellular viruses from host cells (Burleson et al., 1992). Upon repeated cycles of F&T, cells expressing R6S released barely detectable levels of RSP (Figure 6A), confirming that disruption of prM/E interaction inhibited RSP formation. In contrast, similar amounts of RSP were released from cells expressing either wild-type or Triple prME (Figure 6A), indicating that prM/KDELR interaction was dispensable for the formation of viral particles and further suggesting that inhibition of DENV1 and RSP release was the consequence of a trafficking defect.

Next, we studied the role of prM/KDELR interaction in RSP traffic within the ER by immunofluorescence microscopy of cells co-stained with anti-E as well as antibodies labeling ER, *cis*-Golgi and TGN. It has been observed that newly assembled DENV translocate within the ER to accumulate in dilated cisternae oriented toward the *cis*-Golgi (Welsch et al., 2009) and, therefore, we used E protein aggregation as an index of RSP trafficking within the ER. Aggregates were found next to the Golgi apparatus in 50% of cells expressing either wild-type or Triple mutant prME, but were hardly observed in cells stably transfected with R6S (Figures 6B and 6C), suggesting that transport of newly assembled RSP inside ER lumen did not require interaction with KDELR. Similar aggregates were observed in DENV1-infected Vero E6 cells using either a polyclonal antibody against prME or the anti-E monoclonal antibody 4G2 (Figure S6).

Triple Mutant RSP Cannot Exit from ER

To investigate whether interaction with KDELR was required for DENV1 exit from ER, translocation of RSP to the *cis*-Golgi was determined by measuring the percentage of total E protein co-localized with GM130. We found that in cells expressing wild-type prME there was a significantly higher percentage of

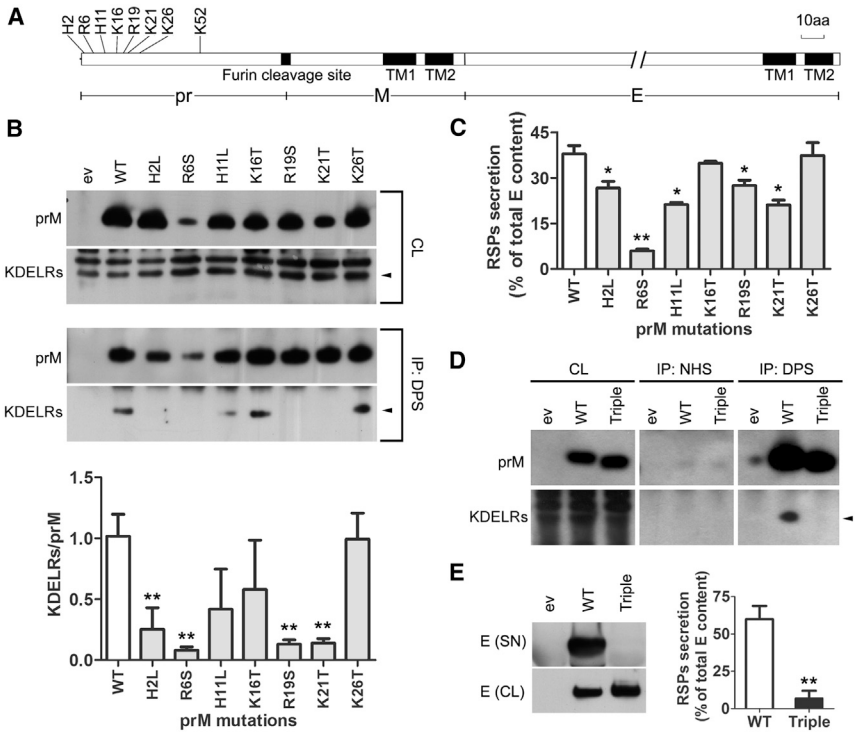

Figure 5. prM/KDELR Interaction Is Dependent on Three Key Residues

(A) Diagram highlighting positively charged amino acids (aa) clustered at the N terminus of prM-DENV1.

(B) Substitutions at H2, R6, R19, and K21 significantly reduced the ability of prM to bind KDELR in transfected 293T cells; wild-type (WT) and empty vector (ev) served as positive and negative controls, respectively. Cell lysates (CL) were subjected to coIP using dengue patient serum (DPS). prM and KDELR were detected by WB in CL or IP pellets (upper). Densitometric ratios of precipitated KDELR/prM are shown as means ± SD (n = 3; lower).

(C) Substitutions at H2, R6, R19, and K21 of prM-DENV1 reduced RSP secretion from 293T cells. E protein in supernatants (SN) and CL was depicted by WB, quantified by densitometry and RSPs secretion was expressed as the percentage of E protein detected in SN relative to total content (SN+CL). Results are means ± SD of triplicate measurements from three independent experiments.

(D) A triple prME mutant (H2L-R19S-K21T; Triple) was completely devoid of interaction with KDELR (no coIP with DPS).

(E) RSP were not secreted from cells transfected with Triple mutant. RSPs release in the SN was assessed by visualizing dengue E protein by WB (left). Blots were quantified by densitometry and RSPs secretion was expressed as the percentage of E protein detected in the supernatant relative to the total amount (SN+CL). Results are means ± SD (n = 3, right). *p < 0.05; **p < 0.001 versus WT.

E protein co-localized with GM-130 with respect to R6S, which does not form RSP and served as the negative control, and Triple mutant, which behaved indistinguishably from R6S (Figures 6B and 6D). Furthermore, similar results were obtained when co-localization of E protein with a TGN marker was measured, with R6S and Triple mutant exhibiting a 50% reduction with respect to wild-type prME (Figures 6B and 6E). These results indicate that RSP of Triple prME were not efficiently translocated from the ER to the Golgi apparatus.

The involvement of KDELR in DENV1 exit from ER was further studied by monitoring intracellular dimerization of E protein. It has been reported that DENV glycoprotein prME undergoes a conformational change in the Golgi apparatus, possibly caused by luminal acidification, which leads to the formation of E homodimers (Li et al., 2008; Yu et al., 2008). RSP released by F&T showed that the percentage of E/E homodimers was 3- to 4-fold higher in cells expressing wild-type prME in comparison to Triple prME, which behaved in similar fashion to R6S (Figure 6F), corroborating immunofluorescence observations (Figures 6B–6D).

Finally, because translocation from ER to Golgi is known to be mediated by vesicular transport (Antonny and Schekman, 2001), we investigated whether KDELR/prME interaction also affected the formation of RSP-containing vesicles. Expression of the different prME constructs did not change the distribution of ERGIC53 (Figure 7A), which cycles between ER and Golgi (Schindler et al., 1993) and was used as marker of trafficking between these two organelles. RSP-containing vesicles (puncta co-stained with anti-E and anti-ERGIC53) were rarely detected in cells expressing Triple mutant or R6S prME, but readily observed with wild-type prME (Figure 7B).

DISCUSSION

We provide here several lines of evidence to propose a role for KDELR in supporting the early steps of intracellular trafficking of both DENV1 and DENV1/RSP, namely their translocation from the ER to the *cis*-Golgi compartment. KDELR interact with DENV1 through three positive charged amino acids at the N terminus of prM protein and DENV1/RSP egress is inhibited either by downregulation of KDELR, sequestration of KDELR in the Golgi, or by disruption of prM/KDELR interaction. Our results further indicate that interaction with KDELR is important for DENV1/RSP to be licensed as cargo of trafficking vesicles leaving the ER. Because KDELR were not required for constitutive secretion of soluble proteins, these findings demonstrate that intracellular transport of DENV/RSP is regulated by interaction with specific cellular factors and identify KDELR as an essential component of this process.

The term receptor in virology refers to host plasma membrane proteins that recognize viral structural components, triggering receptor-mediated endocytosis of the bound pathogen (Mercer et al., 2010). The process of DENV transportation from ER to Golgi apparatus shares several similarities to viral entry. In both processes viruses can be viewed as cargo that is translocated from a neutral environment (extracellular milieu or ER) to an acidic compartment (endosome or Golgi), needs to overcome a lipid membrane barrier to reach its final destination (cytoplasm

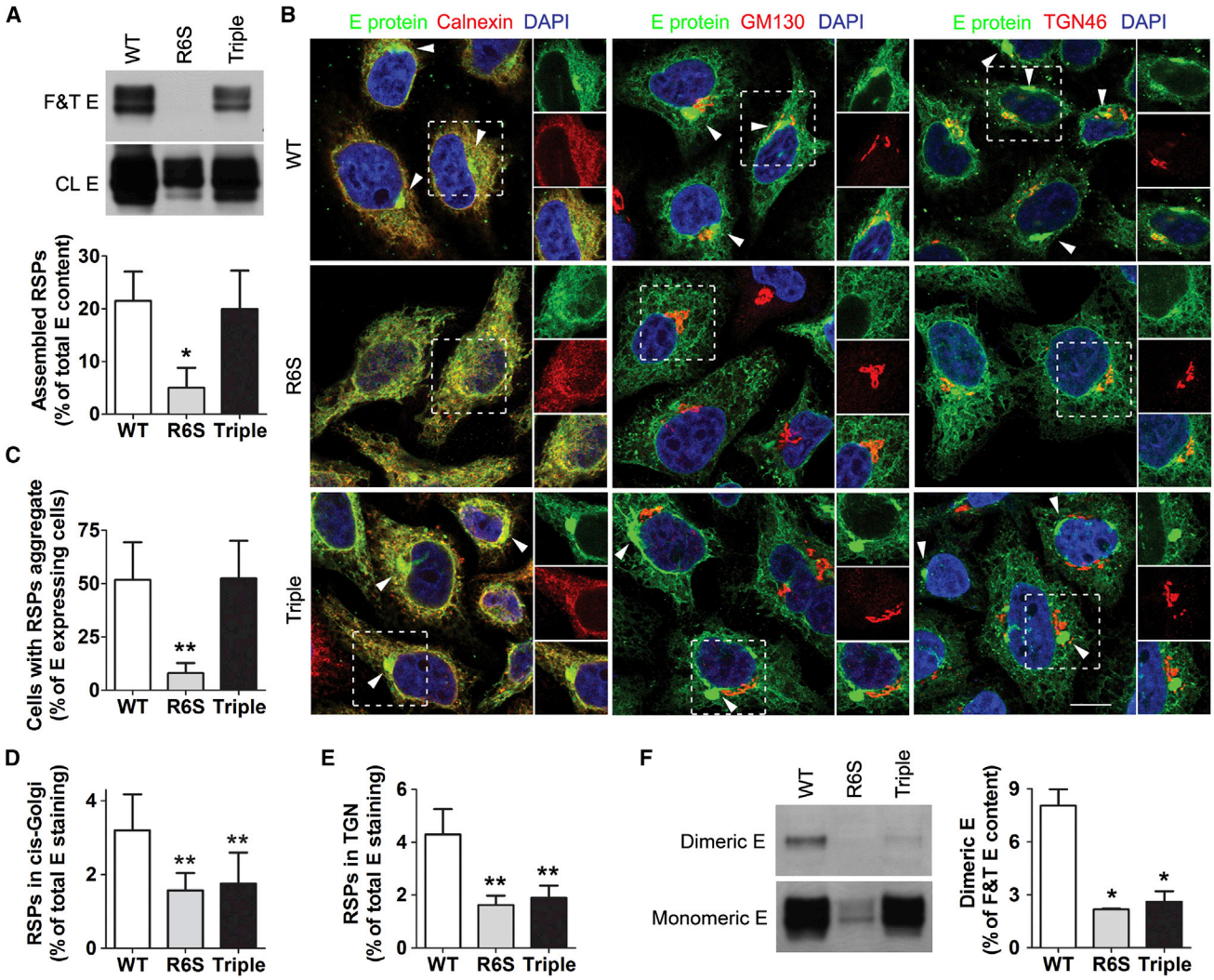

Figure 6. RSP Formed by the Triple Mutant Do Not Exit the ER

(A) Triple prME mutant (Triple), but not R6S-prME (R6S), assembled RSP. Cells were subjected to cycles of freeze-and-thaw (F&T) and E protein detected in cell lysates (CL) or in supernatants after F&T was analyzed by WB (upper). The percentage of E released by F&T relative to the total amount (CL+F&T) was used as index of RSP formation. Results are means ± SD (n = 3, lower).

(B) E protein localization in cells expressing wild-type (WT), Triple or R6S prME. Cells were co-stained with anti-E (4G2, green) and markers for various compartments (red): anti-calnexin (ER), anti-GM130 (*cis*-Golgi), anti-TGN46 (trans-Golgi network, TGN). Arrowheads indicate aggregates of E protein. Scale bar represents 10 μm.

(C) The percentage of cells containing aggregates was quantified from at least three independent experiments. Results are means ± SD of the indicated number of cells (WT, n = 3152; R6S, n = 2901; Triple, n = 2842).

(D and E) Quantification of E staining within Golgi apparatus. The region labeled with either anti-GM130 or anti-TGN46 was assigned to *cis*-Golgi and TGN, respectively. The percentage of E protein in each Golgi sub-compartment was calculated as described in the Experimental Procedures. Results are means ± SD from at least three independent experiments of the specified number of cells (for *cis*-Golgi: WT = 1238; R6S = 1159; Triple = 1188; for TGN: WT = 1268, R6S = 1209, Triple = 1214).

(F) Reduced dimerization of E protein in Triple mutant. RSP released after F&T were subjected to WB using anti-E antibody (left). The percentage of dimeric form relative to total (dimeric + monomeric) E protein released by F&T is presented as means ± SD (n = 3, right). *$p < 0.01$; **$p < 0.005$ versus WT.

for replication or extracellular milieu for another infection round), and is delivered in the form of trafficking vesicles (Humphries and Way, 2013; Modis, 2013; Rothman and Orci, 1992; Sun et al., 2013). Therefore, KDELR can be considered as intracellular receptors for DENV/RSP trafficking, whose function is akin to the role played by cell surface proteins in mediating viral entry.

Many cellular factors have been shown to be crucial for DENV life cycle (Sessions et al., 2009), but viral-host interactions that assist in secretion of newly formed virions are still unclear and no host receptors mediating secretion of progeny virus are known. Thus, although one study suggested an indirect role of KDELR in early vaccinia virus biogenesis, by recruiting

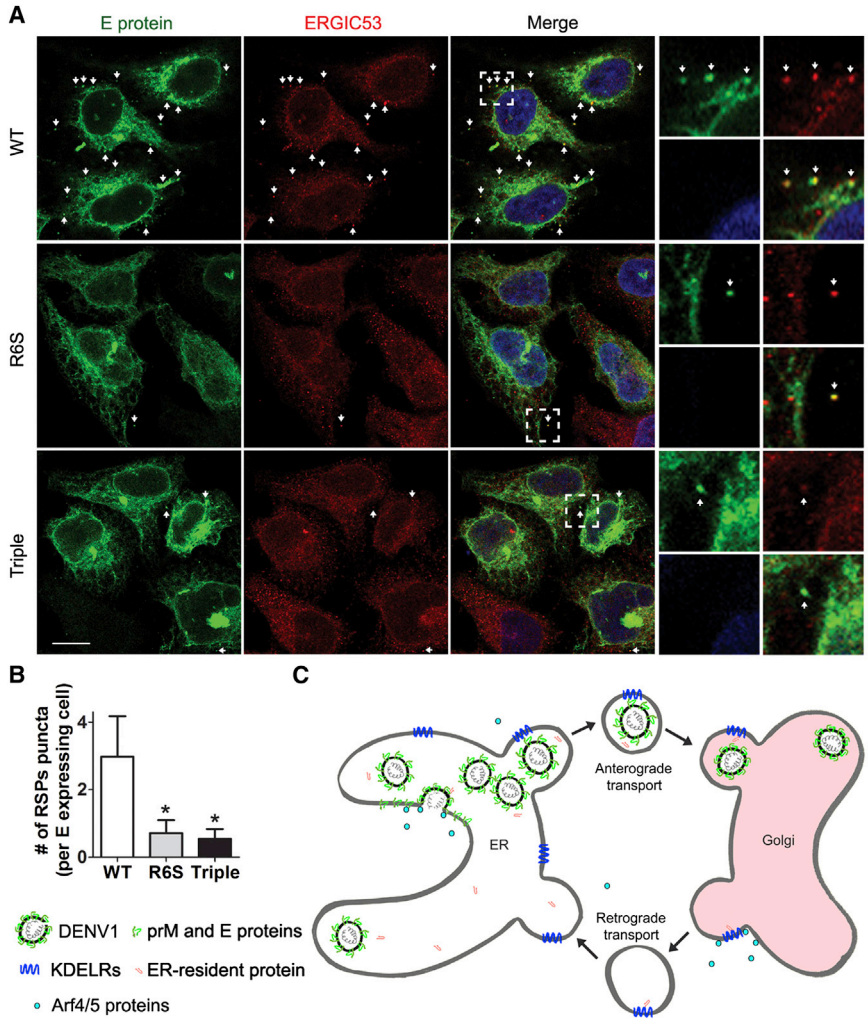

Figure 7. prM/KDELR Interaction Assists Vesicular Transport of DENV from ER to Golgi

(A) Cells expressing wild-type (WT), Triple or R6S prME were co-stained with anti-E (green) and anti-ERGIC53 (red). Puncta labeled with anti-E and anti-ERGIC53 (arrows) were rarely detected in cells expressing Triple and R6S. Scale bar represents 10 μm.

(B) Quantification of puncta co-stained with anti-E and anti-ERGIC53. Results are means ± SD of the specified number of cells from at least three independent experiments (WT, n = 1203; R6S, n = 1184; Triple, n = 1231). *$p < 0.005$ versus WT.

(C) Working model depicting the role of KDELR in DENV transport. Newly formed virions assembled in the ER exploit KDELR as luminal receptor to be sorted as cargo of vesicles that reach the Golgi, where they dissociate to allow KDELR to retrieve ER resident proteins and become available for more rounds of transport. The precise molecular events regulating interactions of DENV with Arf4+5 and their final trafficking remain to be elucidated.

coatomer, their impact on intracellular transport was not investigated (Zhang et al., 2009). Similarly, the reduction of DENV2 replication associated with KDELR downregulation had been ascribed to decreased cell surface expression of protein disulphide isomerase, which has been proposed to function as an additional DENV receptor (Wan et al., 2012). Our data define a receptor role for KDELR in DENV egress, although it has to be acknowledged that depletion of KDELR in Vero E6 cells reduced viral titer by less than one order of magnitude. Clearly, additional, compensatory factors may assist trafficking of DENV from ER to Golgi, as indicated also by the lack of interaction between DENV4 and KDELRs. Further studies will be needed to identify intracellular receptors for DENV4 as well as for other flaviviruses.

It has been demonstrated that, on immature DENV, prM sits on top of E protein to protect it from the acidic environment along the secretory pathway (Zhang et al., 2003). This topology makes prM more accessible to interactions with host cellular proteins. However, the location of the key amino acid residues mutated in our experiments is different, with R6 facing E protein, while H2, R19, and K21 are positioned on the outside face (Li et al., 2008). This is consistent with our observation that mutation of R6 disrupted interaction with E and prevented assembly of RSP, whereas substitutions of H2, R19, and K21 abolished interaction with KDELR and perturbed RSP trafficking. Sequence alignment shows that a similar cluster of positively charged amino acid is present in DENV1–3 serotypes, whereas DENV4 exhibits non-basic substitutions at residues H2 and H11. This difference correlates with the inability of DENV4 to pull down KDELRs and be affected by KDELR depletion. In keeping with our working model, we found that secretion of WNV, which lacks a high proportion of positively charged amino acids at the N terminus of prM protein, was also unaffected by treatment with siRNAs targeting KDELR. As the acidic pH in the Golgi is closer to the p*I* of positively charged amino acids, it is tempting to speculate that this environment may facilitate dissociation of prM/KDELR complexes by reducing their binding affinity. In contrast, the canonical KDEL motif is more negatively charged (Wilson et al., 1993) and this difference may underlie the cargo switching that allows retrieving of resident ER proteins from Golgi.

The finding that DENV4 was unaffected by KDELR depletion was surprising. We had previously shown that release of DENV4 was inhibited by knocking down Arf4+5 (Kudelko et al., 2012), which would result in sequestration of KDELR in the *cis*-Golgi and, therefore, reduce their availability for DENV4 trafficking. It is logical to postulate that DENV4 may interact in the ER with an additional intracellular receptor in an Arf4+5-dependent manner and be able to translocate along the secretory pathway even when KDELRs were downregulated. Thus, trafficking of flaviviruses may require a specific complement of factors for different viruses and/or strains. It should be pointed out

that, although the Triple mutant was mainly localized in the ER, it was still able to pull down both Arf4 and Arf5, confirming that binding to Arf4+5 and KDELR in the ER are independent events. Arf4+5 are localized at both Golgi and ER (Duijsings et al., 2009) and may play two crucial roles for DENV secretion, by being involved in KDELR recycling and interacting with prM protein. Further experiments will be required to ascertain the precise location and role of class II Arf/prM interaction in DENV trafficking.

The function of prM in DENV biology is attracting more attention. Thus, prM has been recently shown to interact with the light chain Tctex-1 of dynein and play a role in late stages of virus replication (Brault et al., 2011). We demonstrate here that prM interacts with KDELR during virus secretion. Our working hypothesis is that DENV1–3 use unoccupied KDELR, which are recognized by a binding motif in the N terminus of prM, to exit the ER as cargo of vesicles en route to the Golgi apparatus (Figure 7C). We had previously characterized the function of class II Arf proteins in DENV/RSP egress (Kudelko et al., 2012). Simultaneous depletion of Arf4+5 efficiently sequester intracellular KDELR in the Golgi and, therefore, it is logical to postulate that both factors converge on the same pathway to inhibit DENV/RSP secretion (Figure 7C). However, results with DENV4 and WNV suggest that additional host proteins are specifically involved in sorting flaviviruses through late secretory compartments and assisting their release from infected cells. In recent years, evidence has accumulated to suggest that, besides their well-established function in retrieving chaperones, KDELR can be activated by cargo to trigger signaling pathways that regulate anterograde and retrograde traffic (Giannotta et al., 2012; Pulvirenti et al., 2008). Specifically, it has been proposed that KDELRs recognize chaperones that are carried by ER vesicles en route to Golgi (Cancino et al., 2013). It is tempting to speculate, therefore, that during DENV1–3 biogenesis, newly formed virions bind to KDELR to activate cell signaling pathways that facilitate their translocation to the Golgi.

EXPERIMENTAL PROCEDURES

Cells, viruses, antibodies, and siRNA experiments are described in the Supplemental Experimental Procedures. Primers used for RT-PCR, GST pull-down, and site-directed mutagenesis are shown in Tables S1, S2, and S3, respectively.

Protein Analysis and RSP Quantification

Gel electrophoresis and WB analysis were carried out as previously described (Kudelko et al., 2012) To quantify RSP secretion, the area and mean luminescence signals detected by WB in supernatants (SN) and cellular lysates (CL) were measured by densitometry using Image Quant TL (Thermo Fisher). For each condition, the relative amount of secreted RSP (E signal in SN) was calculated as the percentage of total signal ($E_{SN}/E_{SN}+E_{CL}$).

Virus Infection Experiments

Viral stocks of DENV1-4 and WNV were titrated by determining the tissue culture infective dose 50% ($TCID_{50}$/ml) in Vero E6 cells challenged with 10-fold serial dilutions of infectious supernatants for 90 min at 37°C. Cells were subsequently incubated in DMEM with 2.5% fetal calf serum. At 5–7 days postinfection for DENV1–3 and 3–5 days postinfection for DENV4 and WNV, culture supernatant was removed and cell monolayers were fixed in 4% formaldehyde. The percentage of cytopathic effects was used to calculate the viral titer.

For measurements of progeny virus production, viral RNA was extracted from culture supernatants and quantified by real-time RT-PCR (see the Supplemental Experimental Procedures). The amount of viral RNA transcripts was then calculated by generating a standard curve with 10-fold dilutions of RNA isolated from a known amount of DENV1 stock and expressed as $TCID_{50}$/ml, as described above.

GST Pull-Down Assay

Fragments of the prM sequence of DENV1 were amplified by PCR (Table S2). Amplicons were subcloned in frame into the bacterial expression vector pGEX-4T-1 to produce N-terminal tagged GST constructs (see the Supplemental Experimental Procedures). Twenty micrograms of each purified protein bound to sepharose 4B-glutathione beads was mixed with lysates of HeLa cells stably expressing cMyc-KDELR, incubated overnight at 4°C, and extensively washed before eluting bound proteins, according to the manufacturer's instructions, for WB analysis.

Coimmunoprecipitation

Sub-confluent monolayers of HeLa-prME-DENV1 or 293T cells transfected with the specified constructs were lysed on ice for 30 min with 1ml RIPA buffer, supplemented with freshly added 1 mM PMSF and protease inhibitors cocktail. Cell debris were removed by centrifugation at 13,000 rpm for 15 min at 4°C and lysates were pre-cleared by incubation with 30 μl of 50% protein G sepharose beads (Amersham Pharmacia) for 1 hr. Pre-cleared lysates (400 ul) were then incubated for 2 hr at 4°C with additional 30 μl of 50% protein G sepharose beads previously treated with either specific antibodies or control IgGs. Beads were then pelleted by centrifugation at 13,000 rpm for 30 s at 4°C and bound proteins were eluted by boiling in gel loading buffer, separated by electrophoresis and analyzed with WB.

Freeze-and-Thaw Assay

For subcellular fractionation (Xu et al., 1997), sub-confluent HeLa cells stably expressing either wild-type prME-DENV1 or the specified mutants were first detached in PBS plus 5 mM EDTA at 37°C for 5 min and washed three times on ice with PBS supplemented with 1 mM EGTA. Cells were then re-suspended in a buffer containing 10% wieght/vol sucrose, 20 mM Tris HCl, 150 mM NaCl, 10 mM magnesium acetate, 1 mM EGTA (pH 7.6) supplemented with freshly added 1 mM PMSF and protease inhibitors cocktail, and then subjected to eight cycles of freeze (dry ice) and thaw (37°C water bath), 1 min each step. Nuclei and cellular debris were removed by a short (5 s) spin at maximum speed in a bench-top centrifuge at 4°C. Supernatants were collected and centrifuged for 30 min at maximum speed at 4°C to pellet the membrane fraction. The final supernatants, containing newly formed RSP, were analyzed with WB.

Fluorescence Microscopy

For fluorescence microscopy, cells grown on glass coverslips were fixed, permeabilized, and incubated with primary antibodies (see the Supplemental Experimental Procedures). Samples were then probed with appropriate secondary antibodies conjugated with fluorescein isothiocyanate or Texas Red (both from Life Technologies). Nuclei were stained with DAPI and coverslips were mounted on glass slides for image acquisition using either an Axio Observer Z1 inverted microscope or an LSM 700 confocal microscope (Carl Zeiss).

Quantitative Analysis of Fluorescent Images

To extract and quantify cells stained with the viral E protein, we developed a specific protocol, "Stained cells," in the ICY software (http://icy.bioimageanalysis.org) (de Chaumont et al., 2012). To extract and quantify cells that contained RSP aggregates, we developed a separate protocol, "Cells with aggregates," in the ICY software. Details of these protocols are provided in the Supplemental Experimental Procedures.

To determine RSP localization in the Golgi apparatus, weighted co-localization coefficients of E with Golgi markers were computed using the ZEN2011 co-localization coefficient software (Carl Zeiss). The sums of intensities of pixels corresponding to anti-E (So) and to co-staining with anti-E and either *cis*-Golgi or TGN marker (Sc) were computed and then weighted co-localization coefficients, which are equal to the ratio of Sc to So, were used to

represent the percentage of RSP translocated to either *cis*-Golgi or TGN. To determine the number of RSP-containing vesicles, we manually counted (in blind) puncta co-labeled with anti-E and anti-ERGIC that were adjacent to perinuclear E-staining. The total number of double-labeled puncta per field was then calculated, divided by the number of cells expressing E protein and displayed as the number of puncta per cell. Data sets for quantitative analysis were acquired from an average of 40–50 fields from four to five independent experiments for each condition.

Statistical Analysis

Results are shown as means ± SD. Statistical significance was analyzed by the Student's unpaired t test, with a confidence limit for significance set at 0.05 or less.

SUPPLEMENTAL INFORMATION

Supplemental Information includes Supplemental Experimental Procedures, six figures, and three tables and can be found with this article online at http://dx.doi.org/10.1016/j.celrep.2015.02.021.

AUTHOR CONTRIBUTIONS

M.Y.L., K.K., Y.L.S., and M.K. performed the experiments on prM/KDELR interaction. M.Y.L., J.S.Z., and K.S. performed the experiments with replicable dengue viruses. T.L. and J.-C.O.-M. designed the software for co-localization analysis. C.F.Q. produced and purified the monoclonal antibody. M.G., J.-C.O.-M., R.B., and P.G.W. analyzed the results. R.B. and P.G.W. prepared and revised the manuscript.

ACKNOWLEDGMENTS

HKU-Pasteur Research Pole is a member of the Institut Pasteur International Network. We thank V. Malhotra (Center for Genomic Regulation, Barcelona) for the gift of soluble horseradish peroxidase construct; R. Gijsbers (Katholieke Universiteit, Leuven) for the retroviral vector; P. Despres (Institut Pasteur, Paris) for the anti-E antibody 4E11; P. Buchy (Institut Pasteur du Cambodge, Phnom Penh) and M. Dupont-Rouzeyrol (Institut Pasteur de Nouvelle-Calédonie, Nouméa) for mouse anti-prME antibody and dengue patients sera; S. Nopporn (Chiang Mai University, Thailand) for anti-prM antibody prM-6.1; P.H.M. Leung (The Hong Kong Polytechnic University, Hong Kong SAR) for the anti-prME polyclonal antibody; J. Guo and the Faculty Core Facility of the LKS Faculty of Medicine of the University of Hong Kong for support with confocal microscopy; P. Chavrier (Institut Curie, Paris), S. Sanyal (HKU-Pasteur Research Pole), and C. Zurzolo (Institut Pasteur, Paris) for critical comments; and members of HKU-Pasteur for useful discussion and technical advice. This work was funded by RFCID (grant #10091312 to P.G.W.), Institut Pasteur International Network (ACIP A-12-10 to P.G.W. and M.G.), BNP Paribas CIB (to R.B.), and ANR-10-INBS-04-06 FranceBioImaging and ANR-10-LABX-62-IBEID (to T.L. and J.-C.O.-M.). M.Y.L. was supported in part by The University of Hong Kong through a postgraduate scholarship and by the LKS Faculty of Medicine through a Research Postgraduate Student Exchange Scheme. T.L. was funded by a Roux fellowship from Institut Pasteur.

Received: April 23, 2014
Revised: October 16, 2014
Accepted: February 4, 2015
Published: March 5, 2015

REFERENCES

Antonny, B., and Schekman, R. (2001). ER export: public transportation by the COPII coach. Curr. Opin. Cell Biol. *13*, 438–443.

Bard, F., Casano, L., Mallabiabarrena, A., Wallace, E., Saito, K., Kitayama, H., Guizzunti, G., Hu, Y., Wendler, F., Dasgupta, R., et al. (2006). Functional genomics reveals genes involved in protein secretion and Golgi organization. Nature *439*, 604–607.

Brault, J.B., Kudelko, M., Vidalain, P.O., Tangy, F., Desprès, P., and Pardigon, N. (2011). The interaction of flavivirus M protein with light chain Tctex-1 of human dynein plays a role in late stages of virus replication. Virology *417*, 369–378.

Burleson, P.G., Chambers, T.M., and Wiedbrauk, D.L. (1992). Virology: A Laboratory Manual (San Diego, CA: Academic Press).

Campbell, G.L., Marfin, A.A., Lanciotti, R.S., and Gubler, D.J. (2002). West Nile virus. Lancet Infect. Dis. *2*, 519–529.

Cancino, J., Jung, J.E., and Luini, A. (2013). Regulation of Golgi signaling and trafficking by the KDEL receptor. Histochem. Cell Biol. *140*, 395–405.

Chen, Y., Maguire, T., Hileman, R.E., Fromm, J.R., Esko, J.D., Linhardt, R.J., and Marks, R.M. (1997). Dengue virus infectivity depends on envelope protein binding to target cell heparan sulfate. Nat. Med. *3*, 866–871.

Courageot, M.P., Frenkiel, M.P., Dos Santos, C.D., Deubel, V., and Desprès, P. (2000). Alpha-glucosidase inhibitors reduce dengue virus production by affecting the initial steps of virion morphogenesis in the endoplasmic reticulum. J. Virol. *74*, 564–572.

D'Souza-Schorey, C., and Chavrier, P. (2006). ARF proteins: roles in membrane traffic and beyond. Nat. Rev. Mol. Cell Biol. *7*, 347–358.

de Chaumont, F., Dallongeville, S., Chenouard, N., Hervé, N., Pop, S., Provoost, T., Meas-Yedid, V., Pankajakshan, P., Lecomte, T., Le Montagner, Y., et al. (2012). Icy: an open bioimage informatics platform for extended reproducible research. Nat. Methods *9*, 690–696.

Duijsings, D., Lanke, K.H.W., van Dooren, S.H.J., van Dommelen, M.M.T., Wetzels, R., de Mattia, F., Wessels, E., and van Kuppeveld, F.J.M. (2009). Differential membrane association properties and regulation of class I and class II Arfs. Traffic *10*, 316–323.

Giannotta, M., Ruggiero, C., Grossi, M., Cancino, J., Capitani, M., Pulvirenti, T., Consoli, G.M., Geraci, C., Fanelli, F., Luini, A., and Sallese, M. (2012). The KDEL receptor couples to Gαq/11 to activate Src kinases and regulate transport through the Golgi. EMBO J. *31*, 2869–2881.

Guzman, M.G., Halstead, S.B., Artsob, H., Buchy, P., Farrar, J., Gubler, D.J., Hunsperger, E., Kroeger, A., Margolis, H.S., Martínez, E., et al. (2010). Dengue: a continuing global threat. Nat. Rev. Microbiol. *8* (*12, Suppl*), S7–S16.

Hsu, V.W., Shah, N., and Klausner, R.D. (1992). A brefeldin A-like phenotype is induced by the overexpression of a human ERD-2-like protein, ELP-1. Cell *69*, 625–635.

Humphries, A.C., and Way, M. (2013). The non-canonical roles of clathrin and actin in pathogen internalization, egress and spread. Nat. Rev. Microbiol. *11*, 551–560.

Kudelko, M., Brault, J.B., Kwok, K., Li, M.Y., Pardigon, N., Peiris, J.S., Bruzzone, R., Desprès, P., Nal, B., and Wang, P.G. (2012). Class II ADP-ribosylation factors are required for efficient secretion of dengue viruses. J. Biol. Chem. *287*, 767–777.

Kuhn, R.J., Zhang, W., Rossmann, M.G., Pletnev, S.V., Corver, J., Lenches, E., Jones, C.T., Mukhopadhyay, S., Chipman, P.R., Strauss, E.G., et al. (2002). Structure of dengue virus: implications for flavivirus organization, maturation, and fusion. Cell *108*, 717–725.

Lewis, M.J., and Pelham, H.R. (1990). A human homologue of the yeast HDEL receptor. Nature *348*, 162–163.

Lewis, M.J., and Pelham, H.R. (1992a). Ligand-induced redistribution of a human KDEL receptor from the Golgi complex to the endoplasmic reticulum. Cell *68*, 353–364.

Lewis, M.J., and Pelham, H.R. (1992b). Sequence of a second human KDEL receptor. J. Mol. Biol. *226*, 913–916.

Li, L., Lok, S.M., Yu, I.M., Zhang, Y., Kuhn, R.J., Chen, J., and Rossmann, M.G. (2008). The flavivirus precursor membrane-envelope protein complex: structure and maturation. Science *319*, 1830–1834.

Limjindaporn, T., Wongwiwat, W., Noisakran, S., Srisawat, C., Netsawang, J., Puttikhunt, C., Kasinrerk, W., Avirutnan, P., Thiemmeca, S., Sriburi, R., et al. (2009). Interaction of dengue virus envelope protein with endoplasmic reticulum-resident chaperones facilitates dengue virus production. Biochem. Biophys. Res. Commun. *379*, 196–200.

Lindenbach, B.D., and Rice, C.M. (2001). Flaviviridae: the viruses and their replication. In Fields virology (Philadelphia, PA: Lippincott Williams & Wilkins), pp. 991–1041.

Mercer, J., Schelhaas, M., and Helenius, A. (2010). Virus entry by endocytosis. Annu. Rev. Biochem. *79*, 803–833.

Messina, J.P., Brady, O.J., Scott, T.W., Zou, C., Pigott, D.M., Duda, K.A., Bhatt, S., Katzelnick, L., Howes, R.E., Battle, K.E., et al. (2014). Global spread of dengue virus types: mapping the 70 year history. Trends Microbiol. *22*, 138–146.

Modis, Y. (2013). Class II fusion proteins. Adv. Exp. Med. Biol. *790*, 150–166.

Mukhopadhyay, S., Kuhn, R.J., and Rossmann, M.G. (2005). A structural perspective of the flavivirus life cycle. Nat. Rev. Microbiol. *3*, 13–22.

Pryor, M.J., Azzola, L., Wright, P.J., and Davidson, A.D. (2004). Histidine 39 in the dengue virus type 2 M protein has an important role in virus assembly. J. Gen. Virol. *85*, 3627–3636.

Pulvirenti, T., Giannotta, M., Capestrano, M., Capitani, M., Pisanu, A., Polishchuk, R.S., San Pietro, E., Beznoussenko, G.V., Mironov, A.A., Turacchio, G., et al. (2008). A traffic-activated Golgi-based signalling circuit coordinates the secretory pathway. Nat. Cell Biol. *10*, 912–922.

Raykhel, I., Alanen, H., Salo, K., Jurvansuu, J., Nguyen, V.D., Latva-Ranta, M., and Ruddock, L. (2007). A molecular specificity code for the three mammalian KDEL receptors. J. Cell Biol. *179*, 1193–1204.

Rothman, J.E., and Orci, L. (1992). Molecular dissection of the secretory pathway. Nature *355*, 409–415.

Schindler, R., Itin, C., Zerial, M., Lottspeich, F., and Hauri, H.P. (1993). ERGIC-53, a membrane protein of the ER-Golgi intermediate compartment, carries an ER retention motif. Eur. J. Cell Biol. *61*, 1–9.

Sessions, O.M., Barrows, N.J., Souza-Neto, J.A., Robinson, T.J., Hershey, C.L., Rodgers, M.A., Ramirez, J.L., Dimopoulos, G., Yang, P.L., Pearson, J.L., and Garcia-Blanco, M.A. (2009). Discovery of insect and human dengue virus host factors. Nature *458*, 1047–1050.

Sun, E., He, J., and Zhuang, X. (2013). Live cell imaging of viral entry. Curr. Opin. Virol. *3*, 34–43.

Volpicelli-Daley, L.A., Li, Y., Zhang, C.J., and Kahn, R.A. (2005). Isoform-selective effects of the depletion of ADP-ribosylation factors 1-5 on membrane traffic. Mol. Biol. Cell *16*, 4495–4508.

Wan, S.W., Lin, C.F., Lu, Y.T., Lei, H.Y., Anderson, R., and Lin, Y.S. (2012). Endothelial cell surface expression of protein disulfide isomerase activates β1 and β3 integrins and facilitates dengue virus infection. J. Cell. Biochem. *113*, 1681–1691.

Wang, P.G., Kudelko, M., Lo, J., Siu, L.Y., Kwok, K.T., Sachse, M., Nicholls, J.M., Bruzzone, R., Altmeyer, R.M., and Nal, B. (2009). Efficient assembly and secretion of recombinant subviral particles of the four dengue serotypes using native prM and E proteins. PLoS ONE *4*, e8325.

Welsch, S., Miller, S., Romero-Brey, I., Merz, A., Bleck, C.K., Walther, P., Fuller, S.D., Antony, C., Krijnse-Locker, J., and Bartenschlager, R. (2009). Composition and three-dimensional architecture of the dengue virus replication and assembly sites. Cell Host Microbe *5*, 365–375.

Wilson, D.W., Lewis, M.J., and Pelham, H.R. (1993). pH-dependent binding of KDEL to its receptor in vitro. J. Biol. Chem. *268*, 7465–7468.

Xu, Z., Bruss, V., and Yen, T.S. (1997). Formation of intracellular particles by hepatitis B virus large surface protein. J. Virol. *71*, 5487–5494.

Yu, I.M., Zhang, W., Holdaway, H.A., Li, L., Kostyuchenko, V.A., Chipman, P.R., Kuhn, R.J., Rossmann, M.G., and Chen, J. (2008). Structure of the immature dengue virus at low pH primes proteolytic maturation. Science *319*, 1834–1837.

Zhang, Y., Corver, J., Chipman, P.R., Zhang, W., Pletnev, S.V., Sedlak, D., Baker, T.S., Strauss, J.H., Kuhn, R.J., and Rossmann, M.G. (2003). Structures of immature flavivirus particles. EMBO J. *22*, 2604–2613.

Zhang, L., Lee, S.Y., Beznoussenko, G.V., Peters, P.J., Yang, J.S., Gilbert, H.Y., Brass, A.L., Elledge, S.J., Isaacs, S.N., Moss, B., et al. (2009). A role for the host coatomer and KDEL receptor in early vaccinia biogenesis. Proc. Natl. Acad. Sci. USA *106*, 163–168.